

# Direct determination of exchange parameters in $\text{Cs}_2\text{CuBr}_4$ and $\text{Cs}_2\text{CuCl}_4$ : high-field ESR studies

S.A. Zvyagin,<sup>1</sup> D. Kamenskyi,<sup>1,\*</sup> M. Ozerov,<sup>1</sup> J. Wosnitzer,<sup>1,2</sup> M. Ikeda,<sup>3</sup> T. Fujita,<sup>3</sup> M. Hagiwara,<sup>3</sup> A.I. Smirnov,<sup>4</sup> T.A. Soldatov,<sup>5</sup> A.Ya. Shapiro,<sup>6</sup> J. Krzystek,<sup>7</sup> R. Hu,<sup>8,†</sup> H. Ryu,<sup>8,9</sup> C. Petrovic,<sup>8,9</sup> and M.E. Zhitomirsky<sup>10</sup>

<sup>1</sup>*Dresden High Magnetic Field Laboratory (HLD),*

*Helmholtz-Zentrum Dresden-Rossendorf, 01328 Dresden, Germany*

<sup>2</sup>*Institut für Festkörperphysik, TU Dresden, 01068 Dresden, Germany*

<sup>3</sup>*KYOKUGEN, Osaka University, Toyonaka, Osaka 560-8531, Japan*

<sup>4</sup>*P.L. Kapitza Institute for Physical Problems, RAS, 119334 Moscow, Russia*

<sup>5</sup>*Moscow Institute for Physics and Technology, 141700 Dolgoprudnyi, Russia*

<sup>6</sup>*A.V. Shubnikov Institute of Crystallography, RAS, 119333, Moscow, Russia*

<sup>7</sup>*National High Magnetic Field Laboratory, Florida State University, Tallahassee, FL 32310, USA*

<sup>8</sup>*Condensed Matter Physics and Materials Science Department,*

*Brookhaven National Laboratory, Upton, NY 11973, USA*

<sup>9</sup>*Department of Physics and Astronomy, Stony Brook University, Stony Brook, New York 11794-3800, USA*

<sup>10</sup>*Service de Physique Statistique, Magnétisme et Supraconductivité,*

*UMR-E9001 CEA-INAC/UJF, 38054 Grenoble Cedex 9, France*

Spin-1/2 Heisenberg antiferromagnets  $\text{Cs}_2\text{CuCl}_4$  and  $\text{Cs}_2\text{CuBr}_4$  with distorted triangular-lattice structures are studied by means of electron spin resonance spectroscopy in magnetic fields up to the saturation field and above. In the magnetically saturated phase, quantum fluctuations are fully suppressed, and the spin dynamics is defined by ordinary magnons. This allows us to accurately describe the magnetic excitation spectra in both materials and, using the harmonic spin-wave theory, to determine their exchange parameters. The viability of the proposed method was proven by applying it to  $\text{Cs}_2\text{CuCl}_4$ , yielding  $J/k_B = 4.7(2)$  K,  $J'/k_B = 1.42(7)$  K [ $J'/J \simeq 0.30$ ] and revealing good agreement with inelastic neutron-scattering results. For the isostructural  $\text{Cs}_2\text{CuBr}_4$ , we obtain  $J/k_B = 14.9(7)$  K,  $J'/k_B = 6.1(3)$  K, [ $J'/J \simeq 0.41$ ], providing exact and conclusive information on the exchange couplings in this frustrated spin system.

PACS numbers: 75.40.Gb, 76.30.-v, 75.10.Jm

A spin-1/2 Heisenberg antiferromagnet (AF) on a triangular lattice is the paradigmatic model in quantum magnetism, which was intensively studied since Anderson's conjecture of the resonating-valence-bond ground state [1]. In spite of numerous theoretical studies (which predict a rich variety of ground states, ranging from a gapless spin liquid to Néel order), many important details of the phase diagram of triangular-lattice AFs remain controversial or even missing (see, i.e., [2–7]).

In order to test the theory experimentally, a precise information on the spin-Hamiltonian parameters for the materials of interest is highly demanded. The presence of quantum fluctuations makes the accurate description of such systems (first of all, the extraction of the spin Hamiltonian parameters) extremely challenging. One solution to solve this problem is to suppress quantum fluctuations by strong-enough magnetic fields. The system is then in the spin-polarized, magnetically saturated phase. The excitation spectrum above the saturation field,  $H_{\text{sat}}$ , is determined by ordinary magnons, which can be described quantitatively by a simple harmonic spin-wave theory.

Studying the magnon dispersion in quantum magnets above  $H_{\text{sat}}$  by means of inelastic neutron-scattering provides the most straightforward opportunity to extract parameters of the spin Hamiltonian. This method has been used, for instance, to determine the exchange cou-

pling parameters in the triangular-lattice AF  $\text{Cs}_2\text{CuCl}_4$  [8]. Experiments revealed up to 65% difference between the parameters estimated at  $H = 0$  (using the harmonic approximation) and actual values (extracted from measurements at  $H > H_{\text{sat}}$ ), stressing the great importance of high-field experiments. Unfortunately, the applicability of this technique is limited to magnetic fields (of about 15 T) currently available for neutron-scattering experiments.

Electron spin resonance (ESR) offers another means to measure the spin Hamiltonian parameters, directly and with high precision. Similar to the case of neutron scattering, the distinct advantage of the high-field ESR is the availability of *exact* theoretical spin-wave expressions for the magnetically saturated phase. For instance, measurements of ESR spectra in the spin-1 material  $\text{NiCl}_2\cdot 4\text{SC}(\text{NH}_2)_2$  (known as DTN) above the saturation field,  $H_{\text{sat}} = 12.6$  T, allowed to determine the bare single-ion anisotropy and, based on that, to accurately describe the temperature-field phase diagram [9].

In this Letter, we report on a new approach, which combines high-field ESR as a tool to probe the magnon-excitation spectrum above  $H_{\text{sat}}$  and its classical linear spin-wave description, allowing us to accurately determine exchange coupling parameters in a spin-1/2 Heisenberg triangular-lattice AF. This approach is based on the

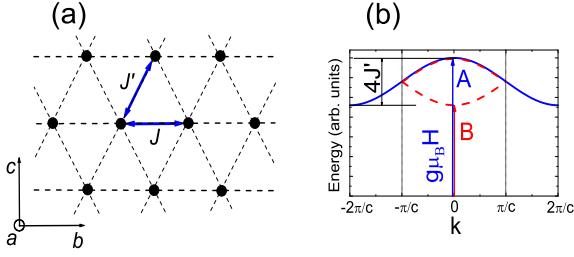


FIG. 1: (Color online) (a) Schematic picture of exchange paths in the  $bc$  plane of CCC and CCB. (b) Dispersion of magnon excitations for a spin-1/2 Heisenberg AF with triangular lattice in the saturated phase for an arbitrary magnetic field. Solid blue line is the dispersion of magnon excitations in the exchange approximation (Eq. 4). The magnon dispersion within the folded Brillouin zone is shown by the dashed red line. Arrows A and B correspond to the observed ESR transitions.

observation of ESR modes of a new type, which becomes possible due to the low-enough crystal symmetry of the studied materials. First, we proved the viability of the proposed technique by applying it to  $\text{Cs}_2\text{CuCl}_4$ . Good agreement between the neutron-scattering [8] and ESR results was obtained. Then, this procedure was employed for the determination of the exchange parameters in the isostructural compound  $\text{Cs}_2\text{CuBr}_4$ , providing the direct answer to the long-standing problem of the spin Hamiltonian parameters of this frustrated compound.

In spite of the recent progress in synthesizing new spin-1/2 triangular-lattice materials (see [10–14] and reference herein) the two compounds,  $\text{Cs}_2\text{CuCl}_4$  and  $\text{Cs}_2\text{CuBr}_4$  (hereafter called CCC and CCB), remain among the most prominent representatives of such kind of frustrated magnets. The  $\text{Cu}^{2+}$  ions in CCC and CCB form a distorted triangular lattice and can be described by the exchange Hamiltonian

$$\mathcal{H} = J \sum_{\langle i,j \rangle} \mathbf{S}_i \cdot \mathbf{S}_j + J' \sum_{\langle i,j' \rangle} \mathbf{S}_i \cdot \mathbf{S}_{j'}, \quad (1)$$

where  $\mathbf{S}_i$ ,  $\mathbf{S}_j$ , and  $\mathbf{S}_{j'}$  are spin-1/2 operators at sites  $i$ ,  $j$ , and  $j'$ , respectively;  $J$  is the interaction constant along the  $b$  direction;  $J'$  is the zig-zag interchain coupling [Fig. 1 (a)]. The orthorhombic crystal structure of CCC corresponds to the space group  $Pnma$  with the room-temperature lattice parameters  $a = 9.769 \text{ \AA}$ ,  $b = 7.607 \text{ \AA}$ , and  $c = 12.381 \text{ \AA}$  [15]. At  $T_N = 0.62 \text{ K}$ , CCC undergoes a transition into helical incommensurate (IC) long-range-ordered state [16]. CCC is in the saturated phase above the critical fields  $H_{\text{sat}} = 8.44, 8.89$  and  $8 \text{ T}$  applied along the  $a$ ,  $b$ , and  $c$  axis, respectively [17]. The exchange interactions were estimated from the mentioned above inelastic neutron-scattering experiments in the saturated phase [8], yielding  $J/k_B = 4.34(6) \text{ K}$  and  $J'/k_B = 1.48(6) \text{ K}$  [ $J'/J = 0.34(2)$ ].

Similar to CCC, the isostructural compound CCB

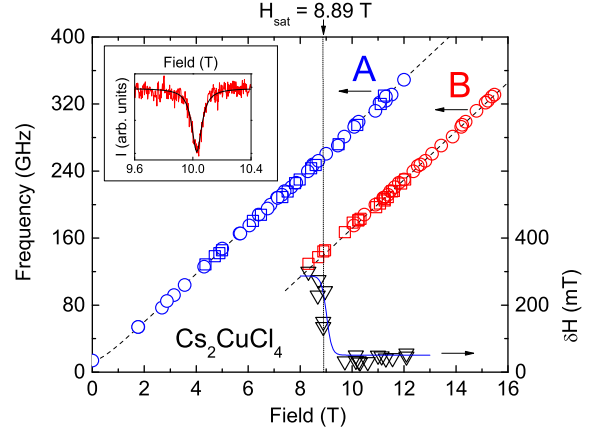


FIG. 2: (Color online) Frequency-field diagram of the ESR excitations in CCC measured at 0.5 K (squares) and 1.5 K (circles). Dashed lines correspond to fit results (see text for details). The linewidth (half width at half maximum) of mode B vs field is shown by triangles; the solid line is a guide for the eye. Inset shows an example of ESR spectrum (mode B) taken at 178.3 GHz ( $T = 0.53 \text{ K}$ ); the solid line corresponds to a Lorentzian fit.

realizes a distorted triangular lattice with the room-temperature lattice parameters  $a = 10.195 \text{ \AA}$ ,  $b = 7.965 \text{ \AA}$ , and  $c = 12.936 \text{ \AA}$  [18]. At  $T_N = 1.4 \text{ K}$ , CCB undergoes a transition into helical IC long-range-ordered state [19, 20]. CCB is in the saturated phase above  $H_{\text{sat}} = 30.71, 30.81$ , and  $28.75 \text{ T}$  applied along the  $a$ ,  $b$ , and  $c$  axis, respectively [21]. Within a classical spin model, the ratio  $J'/J = 0.467$  was estimated [19–21]. On the other hand, results of density-functional calculations suggest  $J'/J \sim 0.5 - 0.65$  [22], while the ratio  $J'/J = 0.74$  was obtained [23] by comparison of the zero-field IC wavenumber in the ordered phase with results of the series expansion method [24].

Single crystals of CCC (CCB) were synthesized by slow evaporation of aqueous solutions of  $\text{CsCl}$  and  $\text{CuCl}_2$  ( $\text{CsBr}$  and  $\text{CuBr}_2$ ). Samples of CCC were from the same batch as in Ref. [25, 26]. Experiments were performed using ESR spectrometers operated in combination with superconducting (KYOKUGEN, HLD, Kapitza Institute), 25 T resistive (NHMFL [27]), and 50 T pulse-field (KYOKUGEN, HLD) magnets. The spectrometer at the Kapitza Institute with a  $^3\text{He}$  insert and 12 T magnet was used for taking spectra down to 0.45 K. Backward wave oscillators, VDI generators (product of Virginia Diodes Inc.), and  $\text{CO}_2$ -pumped molecular laser (product of Edinburgh Instruments Ltd.) were used as sources of mm- and submm-wavelength radiation. In our experiments, the magnetic field was applied along the crystallographic  $b$  axis. 2,2-diphenyl-1-picrylhydrazyl (known as DPPH) was employed as a standard marker for the accurate calibration of the magnetic field.

The frequency-field diagrams of the ESR absorption in

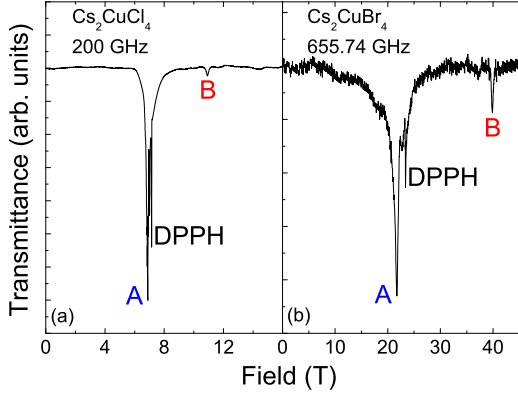


FIG. 3: (Color online) ESR spectra of CCC (a) and CCB (b), taken at frequencies 200 and 655.74 GHz, respectively ( $T = 1.5$  K). DPPH is employed as a standard marker.

CCC at 0.5 and 1.5 K are shown in Fig. 2 by squares and circles, respectively. Two resonance modes of different intensity were observed (Fig. 3, a). The most intensive mode, the mode A, can be described using the equation  $\hbar\omega_A = \sqrt{(g_b\mu_B H)^2 + \Delta_A^2}$ , where  $\hbar$  is the Planck constant,  $\omega$  is the excitation frequency,  $\mu_B$  is the Bohr magneton,  $\Delta_A/(2\pi\hbar) = 14$  GHz and  $g_b = 2.08(2)$  [25]. Above  $H_{sat}$ , the mode A corresponds to the collective excitation of spins with the frequency  $\omega_A \approx g_b\mu_B H/\hbar$  and can be interpreted as uniform  $\mathbf{k} = 0$  precession of spins around the field direction. The much weaker mode B appears at  $H \gtrsim H_{sat}$ . The frequency of this mode can be described empirically using the equation  $\hbar\omega_B = g_b\mu_B H - \Delta_B$  with the same  $g$ -factor,  $g_b = 2.08$ , and  $\Delta_B/(2\pi\hbar) = 119.0(3)$  GHz. The ESR line undergoes a significant broadening approaching  $H_{sat}$  from the high-field end (Fig. 2, triangles), becoming undetectable below 8 T. An example of ESR spectrum (mode B), taken at 178.3 GHz ( $T = 0.53$  K) is shown in the inset of Fig. 2; the solid line corresponds to a Lorentzian fit.

The emergence of two ESR modes in the magnetically saturated state signifies a lower crystal symmetry compared to the one assumed in the simple spin model (1). This is not entirely surprising since the unit cell of CCC is made up of four inequivalent  $\text{Cu}^{2+}$  ions: two on the adjacent  $b$ -chains in the  $bc$  plane and two on the adjacent layer shifted along the  $b$  and  $c$  axes by a half of lattice constant [16]. One single copper layer is described by the exchange Hamiltonian (1). On the other hand, the crystal symmetry of CCC allows the Dzyaloshinskii-Moriya (DM) interaction for all nearest-neighbor spin bonds in a single copper layer:

$$\hat{\mathcal{H}}_{DM} = \sum_i \sum_{n=1}^3 \mathbf{D}_n \cdot [\mathbf{S}_i \times \mathbf{S}_{i+\delta_n}] , \quad (2)$$

where the lattice vectors  $\delta_n$  are chosen as  $\delta_1 = (0, b, 0)$ ,

$\delta_{2,3} = (0, \pm b/2, c/2)$ . The DM vectors compatible with the space group of the crystal are given by

$$\begin{aligned} \mathbf{D}_1 &= (D_a, 0, (-1)^{i_c} D_c) , \\ \mathbf{D}_{2,3} &= (\pm D'_a, (-1)^{i_c} D'_b, \pm (-1)^{i_c} D'_c) , \end{aligned} \quad (3)$$

where  $i_c$  is the chain index in the  $c$ -direction (see [5] for further details on the DM interactions in CCC). So far, experiments on CCC gave estimates for three DM parameters:  $D'_a/J \sim 5\%$  [8] and  $D_{a,c}/J \sim 10\%$  [25, 28].

The reduced translational symmetry of the copper layers in CCC (CCB) revealed by the staggered DM vectors (3) leads to the folding of the Brillouin zone of a simple triangular Bravais lattice. As a result, the ESR transitions are allowed not only for  $\mathbf{k} = 0$  (mode A) but also for  $k_c = 2\pi/c$  (exchange mode B). A detailed analysis of the excitation spectrum for the spin Hamiltonian given by the sum of (1) and (2) is presented in the Supplemental Material [29]. Here, we resort to a simpler line of arguments valid in the case of small DM interaction. We just neglect the effect of the DM terms (2) on the magnon energy. Then, the dispersion of the magnetic excitations for a spin-1/2 AF (1) in the saturated phase is described by

$$\hbar\omega_{\mathbf{k}} = g\mu_B H + J \cos(k_b b) + 2J' \cos(\frac{1}{2}k_b b) \cos(\frac{1}{2}k_c c) - J_0 , \quad (4)$$

where  $J_0 = J + 2J'$ . The difference between the excitation energies of the modes A and B [Fig. 1 (b)] is equal to

$$\hbar\Delta\omega = 4J' . \quad (5)$$

For  $\mathbf{H} \parallel b$ , the above approximate expression can be compared to the exact result [29]:

$$\hbar\Delta\omega = 4\sqrt{(J')^2 + (D'_b)^2} . \quad (6)$$

For this, as well as for other field orientations, the correction from a finite value of the DM interaction is of the order of  $(D'_b/J')^2$  and does not exceed 1–2%. However, a finite value of  $D'_b$  is essential for the observation of mode B: the intensity ratio of the two resonance lines scales as  $(D'_b/J')^2$ , so that the mode B would not be seen for  $D'_b = 0$ . Hence, measurements of the ESR spectra in the saturated phase provide a direct and accurate estimate of  $J'$ .

Knowing  $J'$ , we now can determine  $J$  from the saturation field using the expression

$$g\mu_B H_{sat} = 2J(1 + J'/2J)^2 \quad (7)$$

obtained for the exchange model (1). The correction to Eq. (7) taking the DM interactions into account can be assessed using the expression obtained for  $\mathbf{H} \parallel b$  [29]:

$$g\mu_B H_{sat}^b = 2(J + J') + (J'^2 + D_b'^2)/2J . \quad (8)$$

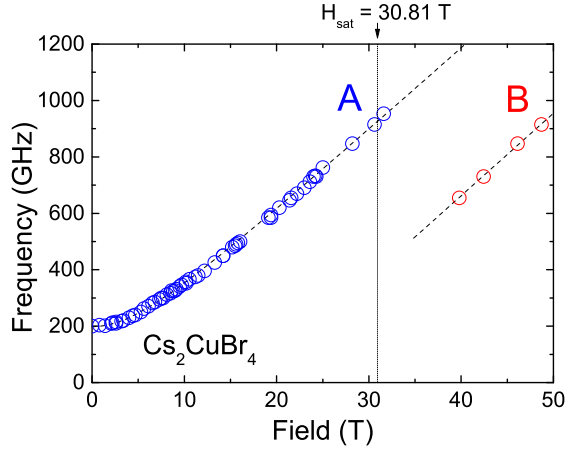


FIG. 4: (Color online) Frequency-field diagram of ESR excitations in CCB ( $T = 1.5$  K). Dash lines correspond to fit results (see the text for details).

Even for  $D'_b \sim 0.1\text{--}0.2J$ , the effect on  $H_{sat}$  for CCC(CCB) can be safely neglected. Thus, using Eqs. (4) and (7),  $g_b = 2.08(2)$ , and  $H_{sat} = 8.89(2)$  T, the exchange coupling parameters for CCC are obtained as  $J/k_B = 4.7(2)$  K and  $J'/k_B = 1.42(7)$  K [ $J'/J = 0.30(3)$ ] [30]. The latter value is in good agreement with the estimate  $J'/J = 0.34(2)$  from the neutron-scattering experiments [8].

Let us also note that in CCC (CCB) the Brillouin-zone folding occurs also in the  $a$  direction perpendicular to the copper layers. By a similar line of arguments this folding yields a further splitting of each mode A and B by  $\delta\omega'' \sim J''$ , where  $J''$  is the interlayer exchange coupling. Since  $J'' = 0.2$  K [8], it is rather difficult to observe such a splitting even in ESR experiments.

Once the viability of the proposed approach is verified, we apply it now to CCB. Compared to CCC,  $H_{sat}$  in CCB is more than 3 times larger, that implies the necessity of ESR measurements in magnetic field above 30 T. Similar to CCC, two ESR modes have been observed at  $H > H_{sat}$  (Fig. 3, b). The frequency-field diagram of ESR excitations in CCB obtained at  $T = 1.5$  K is shown in Fig. 4. The mode A can be described using the equation  $\hbar\omega_A = \sqrt{(g\mu_B H)^2 + \Delta_A^2}$ , where  $g_b = 2.09(2)$  and  $\Delta_A/(2\pi\hbar) = 198$  GHz. The exchange mode B was observed only above  $H_{sat}$ . The mode B can be described by the equation  $\hbar\omega_B = g_b\mu_B H - \Delta_B$ , where  $\Delta_B/(2\pi\hbar) = 507.6$  GHz. Using Eqs. (4) and (7), the exchange coupling parameters for CCB are obtained:  $J/k_B = 14.9(7)$  K and  $J'/k_B = 6.1(3)$  K [ $J'/J = 0.41(4)$ ] [30].

As mentioned, our results for CCC are in a good agreement with those obtained earlier using inelastic neutron-scattering experiments [8]. On the other hand, in the case of CCB a relatively big difference between previously suggested value,  $J'/J = 0.74$  [21], and our result,

$J'/J = 0.41(4)$ , is observed. This difference is of crucial importance for understanding of unusual magnetic properties of CCB. For instance, CCB is a rare example of a spin-1/2 triangular-lattice Heisenberg AF, which exhibits a 1/3 magnetization plateau [19–21]. Numerical diagonalization calculations of a finite-size spin-1/2 Heisenberg AF predicts that the geometric frustration should be sufficiently strong to stabilize the so-called “up-up-down” (UUD) phase, resulting in the emergence of the 1/3 magnetization plateau, in the range  $0.7 \lesssim J'/J \lesssim 1.3$  [31]. On the other hand, density matrix renormalization group calculations predict the 1/3 magnetization plateau even for infinitesimally small  $J'/J$  ratio [32]. Our results suggest that the field-induced UUD phase in spin-1/2 triangle-lattice Heisenberg AF can be realized for the  $J'/J$  ratio, which is much smaller than predicted in Ref. [31]. The obtained spin-Hamiltonian parameters can be of particular importance for a quantitative description of the cascade of field-induced phase transitions observed recently in CCB [33].

In conclusion, the excitation spectra of  $\text{Cs}_2\text{CuCl}_4$  and  $\text{Cs}_2\text{CuBr}_4$  have been probed in magnetic fields up to  $H_{sat}$  and above. Based on the classical linear spin-wave description of the magnon excitation spectrum and high-field magnetization data, the exchange coupling parameters for both compounds were determined. The obtained accurate knowledge is of eminent importance for the understanding of the complex phase diagram of spin-1/2 triangular-lattice Heisenberg AFs. The proposed approach can be used for accurate estimation of exchange parameters of a growing family of spin-1/2 triangular-lattice AFs, including organic compounds (see [10–13] and references herein), those investigations via conventional neutron-scattering techniques is rather challenging. The employment of very high magnetic fields (up to ca 70 T [34, 35] and above [36–38], currently available for pulsed-field magneto-spectroscopy) as well as the rapid progress in the THz techniques makes the proposed method of crucial importance for investigating spin systems with large  $J/k_B$ . The approach has a broader impact and can be potentially used for *any* quantum magnet with reduced (e.g., by the staggered DM interaction) translational symmetry, resulting, as predicted, in emergence of a new exchange mode above  $H_{sat}$ .

This work was supported in part by the DFG. We acknowledge the support of the HLD at HZDR, member of the European Magnetic Field Laboratory. S.A.Z. appreciates the support of the Visiting Professor Program at KYOKUGEN in Osaka University. Work at Brookhaven was supported by the U.S. DOE under Contract No. DE-AC02-98CH10886. C.P. acknowledges the support by the A. von Humboldt Foundation. Work at the Kapitza Institute is supported by Russian foundation for basic research, grant No. 12-02-00557. A portion of this work was performed at the NHMFL, which is supported by NSF Cooperative Agreement No. DMR-1157490, by the



State of Florida, and by the DOE. The authors would like to thank V.N. Glazkov, A.K. Kolezhuk, V.I. Marchenko, S.S. Sosin, and O.A. Starykh for discussions, and S. Miyasaka for the help in orienting the CCB samples.

---

\* Present address: Radboud University Nijmegen, Institute for Molecules and Materials, High Field Magnet Laboratory, 6500 GL Nijmegen, The Netherlands

† Present address: Rutgers Center for Emergent Materials and Department of Physics and Astronomy, Rutgers University, Piscataway, NJ 08854, USA

- [1] P.W. Anderson, *Mater. Res. Bull.* **8**, 153 (1973).
- [2] M.Q. Weng, D.N. Sheng, Z.Y. Weng, and R.J. Bursill, *Phys. Rev. B* **74**, 012407 (2006).
- [3] R. Schmied, T. Roscilde, V. Murg, D. Porras, and J.I. Cirac, *New J. Phys.* **10**, 045017 (2008).
- [4] D. Heidarian, S. Sorella, and F. Becca, *Phys. Rev. B* **80**, 012404 (2009).
- [5] O. A. Starykh, H. Katsura, and L. Balents, *Phys. Rev. B* **82**, 014421 (2010).
- [6] S. Ghamari, C. Kallin, S.S. Lee, and E.S. Sørensen, *Phys. Rev. B* **84**, 174415 (2011).
- [7] A. Weichselbaum and S. R. White, *Phys. Rev. B* **84**, 245130 (2011).
- [8] R. Coldea, D. A. Tennant, K. Habicht, P. Smeibidl, C. Wolters, and Z. Tylczynski, *Phys. Rev. Lett.* **88**, 137203 (2002).
- [9] S. A. Zvyagin, J. Wosnitzer, C. D. Batista, M. Tsukamoto, N. Kawashima, J. Krzystek, V. S. Zapf, M. Jaime, N. F. Oliveira, and A. Paduan-Filho, *Phys. Rev. Lett.* **98**, 047205 (2007).
- [10] M. Yamashita, N. Nakata, Y. Senshu, M. Nagata, H. M. Yamamoto, R. Kato, T. Shibauchi, and Y. Matsuda, *Science* **328**, 1246 (2010); T. Itou, A. Oyamada, S. Maegawa, and R. Kato, *Nat. Phys.* **6**, 673 (2010).
- [11] S. Yamashita, Y. Nakazawa, M. Oguni, Y. Oshima, H. Nojiri, Y. Shimizu, K. Miyagawa, and K. Kanoda, *Nat. Phys.* **4**, 459 (2008); M. Yamashita, N. Nakata, Y. Kasahara, T. Sasaki, N. Yoneyama, N. Kobayashi, S. Fujimoto, T. Shibauchi, and Y. Matsuda, *Nat. Phys.* **5**, 44 (2009).
- [12] K. Kanoda and R. Kato, *Annu. Rev. Condens. Matter Phys.* **2**, 167 (2011).
- [13] B. J. Powell and R. H. McKenzie, *Rep. Prog. Phys.* **74**, 056501 (2011).
- [14] Y. Shirata, H. Tanaka, A. Matsuo, and K. Kindo, *Phys. Rev. Lett.* **108**, 057205 (2012); H. D. Zhou, Cenke Xu, A. M. Hallas, H. J. Silverstein, C. R. Wiebe, I. Umegaki, J.Q. Yan, T. P. Murphy, J.-H. Park, Y. Qiu, J. R. D. Copley, J. S. Gardner, and Y. Takano, *Phys. Rev. Lett.* **109**, 267206 (2012).
- [15] S. Bailleul, D. Svoronos, P. Porchner, and A. Tomas, *Comptes Rendus de l'Academie des Sciences Serie II*, **313**, 1149 (1991).
- [16] R. Coldea, D.A. Tennant, R.A. Cowley, D.F. McMorrow, B. Dorner, and Z. Tylczynski, *J. Phys.: Cond. Matter* **8**, 7473 (1996).
- [17] Y. Tokiwa, T. Radu, R. Coldea, H. Wilhelm, Z. Tylczynski, and F. Steglich, *Phys. Rev. B* **73**, 134414 (2006).
- [18] B. Morosin and E.C. Lingafelter, *Acta Cryst.* **13**, 807 (1960).
- [19] T. Ono, H. Tanaka, O. Kolomiyets, H. Mitamura, T. Goto, K. Nakajima, A. Oosawa, Y. Koike, K. Kakurai, J. Klenke, P. Smeibidl, and M. Meissner, *J. Phys.: Condens. Matter* **16**, S773 (2004).
- [20] T. Ono, H. Tanaka, H. Aruga Katori, F. Ishikawa, H. Mitamura, and T. Goto, *Phys. Rev. B* **67**, 104431 (2003).
- [21] T. Ono, H. Tanaka, O. Kolomiyets, H. Mitamura, F. Ishikawa, T. Goto, K. Nakajima, A. Oosawa, Y. Koike, K. Kakurai, J. Klenke, P. Smeibidl, M. Meissner, R. Coldea, A. D. Tennant, and J. Ollivier, *Progr. of Theor. Phys. Suppl.* **159**, 217 (2005); T. Ono, H. Tanaka, T. Nakagomi, O. Kolomiyets, H. Mitamura, F. Ishikawa, T. Goto, K. Nakajima, A. Oosawa, Y. Koike, K. Kakurai, J. Klenke, P. Smeibidl, M. Meissner, and H.A. Katori, *J. Phys. Soc. Japan*, **74**, 14267 (2005).
- [22] K. Foyevtsova, I. Opahle, Y.-Z. Zhang, H.O. Jeschke, and R. Valentí, *Phys. Rev. B* **83**, 125126 (2011).
- [23] H. Tsujii, C.R. Rotundu, T. Ono, H. Tanaka, B. Andraka, K. Ingersent, and Y. Takano, *Phys. Rev. B* **76**, 060406(R) (2007).
- [24] Z. Weihong, R.H. McKenzie, and R.R.P. Singh, *Phys. Rev. B* **59**, 14367 (1999).
- [25] K.Yu. Povarov, A.I. Smirnov, O.A. Starykh, S.V. Petrov, and A.Ya. Shapiro, *Phys. Rev. Lett.* **107**, 037204 (2011).
- [26] A.I. Smirnov, K.Y. Povarov, S.V. Petrov, and A.Ya. Shapiro, *Phys. Rev. B* **85**, 184423 (2012).
- [27] S.A. Zvyagin, J. Krzystek, P.H.M. van Loosdrecht, G. Dhalenne, and A. Revcolevschi, *Physica B* **346-347**, 1 (2004).
- [28] M.A. Fayzullin, R.M. Eremina, M.V. Eremin, A. Dittl, N. van Well, F. Ritter, W. Assmus, J. Deisenhofer, H.-A. Krug von Nidda, and A. Loidl, *Phys. Rev. B* **88**, 174421 (2013).
- [29] Supplemental Material.
- [30] The largest error source in determining the exchange coupling parameters are the accuracy of the fit and the assumption of the DM contribution (which is less than 10-15 % of  $J$ ). We estimate the accuracy of  $J$  and  $J'$  better than  $\pm 5\%$ .
- [31] S. Miyahara, K. Ogino, and N. Furukawa, *Physica B* **378-380**, 587 (2006).
- [32] R. Chen, H. Ju, H.-C. Jiang, O.A. Starykh, and L. Balents, *Phys. Rev. B* **87**, 165123 (2013).
- [33] N.A. Fortune, S.T. Hannahs, Y. Yoshida, T.E. Sherline, T. Ono, H. Tanaka, and Y. Takano, *Phys. Rev. Lett.* **102**, 257201 (2009).
- [34] S. A. Zvyagin, M. Ozerov, E. Čížmár, D. Kamenskyi, S. Zherlistyn, T. Herrmannsdörfer, J. Wosnitzer, R. Wünsch, and W. Seidel, *Rev. Sci. Instr.* **80**, 073102 (2009).
- [35] S. A. Zvyagin, E. Čížmár, M. Ozerov, J. Wosnitzer, R. Feyerherm, S. R. Manmana, and F. Mila, *Phys. Rev. B* **83**, 060409 (2011).
- [36] H. Nojiri, Y. Shimamoto, N. Miura, M. Hase, K. Uchinokura, H. Kojima, I. Tanaka, and Y. Shibuya, *Phys. Rev. B* **57**, 10276 (1998).
- [37] K. Kindo, S. Takeyama, M. Tokunaga, Y.H. Matsuda, E. Kojima, A. Matsuo, K. Kawaguchi, H. Sawabe, *J. Low Temp. Phys.* **159**, 381 (2010).
- [38] G.V. Boriskov, A.I. Bykov, M.I. Dolotenko, N.I. Egorov, Y.B. Kudasov, V.V. Platonov, V.D. Selemir, O.M. Tatarsenko, *Physics-Uspekhi* **54**, 421 (2011).

## SUPPLEMENTAL MATERIAL

### 2D MODEL FOR $\text{Cs}_2\text{CuCl}_4$

A single plane of copper spins in  $\text{Cs}_2\text{CuCl}_4$  is described by the following spin Hamiltonian [1, 2]:

$$\hat{\mathcal{H}} = \sum_i \left\{ J \mathbf{S}_i \cdot \mathbf{S}_{i+\delta_1} + J' (\mathbf{S}_i \cdot \mathbf{S}_{i+\delta_2} + \mathbf{S}_i \cdot \mathbf{S}_{i+\delta_3}) + \mathbf{D}_1 \cdot [\mathbf{S}_i \times \mathbf{S}_{i+\delta_1}] \right. \\ \left. + \mathbf{D}_2 \cdot [\mathbf{S}_i \times \mathbf{S}_{i+\delta_2}] + \mathbf{D}_3 \cdot [\mathbf{S}_i \times \mathbf{S}_{i+\delta_3}] - g\mu_B \mathbf{H} \cdot \mathbf{S}_i \right\}, \quad (9)$$

where the in-plane nearest-neighbor vectors are defined as  $\delta_1 = (0, b, 0)$  and  $\delta_{2,3} = (0, \pm b/2, c/2)$ , see Fig. 5. From now on we shall use the short-hand notation  $g\mu_B H \rightarrow H$ . The two exchange constants  $J$  and  $J'$  correspond to the chain and zigzag bonds, respectively. The Dzyaloshinskii-Moriya (DM) vector on the chain bonds is

$$\mathbf{D}_1 = (D_a, 0, (-1)^{i_c} D_c), \quad (10)$$

where  $i_c$  is the chain index in the  $c$  direction. On the interchain zigzag bonds one has by symmetry [2]

$$\mathbf{D}_{2,3} = (\pm D'_a, (-1)^{i_c} D'_b, \pm (-1)^{i_c} D'_c). \quad (11)$$

The Hamiltonian (9) is translationally invariant in the direction of spin chains ( $b$ -axis), whereas the alternation of the components of the Dzyaloshinskii-Moriya vectors between the chains leads to a unit cell with two copper atoms.

### HIGH-FIELD TWO-SUBLATTICE STRUCTURE

In antiferromagnets with a uniform arrangement of DM-vectors all spins become parallel to each other at  $H > H_s$ , though this direction generally deviates from the field direction unless  $\mathbf{H} \parallel \mathbf{D}$ . The alternation of the DM vectors in the spin Hamiltonian (9) leads to the presence of two distinct sublattices even in high magnetic fields. It is important that the two sublattices correspond to adjacent chains, whereas the translational symmetry along the chains remains unbroken.

Let us check which components of the DM vectors in (9) are responsible for the above effect and, therefore, play a role in the uniform magnetic resonance. The DM interaction on the chain bonds can be rewritten as

$$\hat{\mathcal{H}}_{DM}^{(1)} = \frac{1}{2} \sum_i \mathbf{D}_1 \cdot [\mathbf{S}_i \times (\mathbf{S}_{i+\delta_1} - \mathbf{S}_{i-\delta_1})]. \quad (12)$$

Its expectation value vanishes for a uniform state along the chains. Hence, the term (12) may contribute to the ESR frequencies only beyond the harmonic approximation and can be safely neglected at high fields. On the zigzag interchain bonds one has to consider separately different components. The contribution from the  $a$  component is

$$\hat{\mathcal{H}}_{DM}^{(2)} = \frac{1}{2} D'_a \sum_i \hat{\mathbf{a}} \cdot [\mathbf{S}_i \times (\mathbf{S}_{i+\delta_2} - \mathbf{S}_{i-\delta_2} - \mathbf{S}_{i+\delta_3} + \mathbf{S}_{i-\delta_3})]. \quad (13)$$

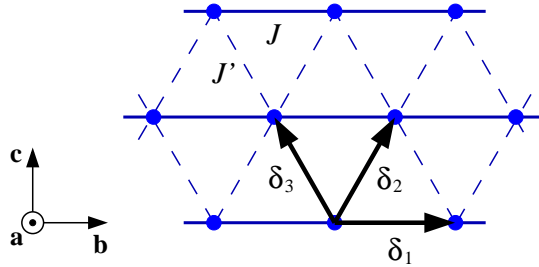


FIG. 5: The orthorhombically distorted triangular lattice.

It again vanishes for a translationally invariant state along the chains. The contribution from the  $b$  component is

$$\hat{\mathcal{H}}_{DM}^{(3)} = \frac{1}{2} D'_b \sum_i \hat{\mathbf{b}} \cdot [\mathbf{S}_i \times (\mathbf{S}_{i+\delta_2} + \mathbf{S}_{i-\delta_2} + \mathbf{S}_{i+\delta_3} + \mathbf{S}_{i-\delta_3})] . \quad (14)$$

This contribution does not vanish and generates a staggered field along the  $b$  direction responsible for the two sublattice structure, which survives in strong magnetic field. Finally, the contribution from the  $c$  component is

$$\hat{\mathcal{H}}_{DM}^{(4)} = \frac{1}{2} D'_c \sum_i \hat{\mathbf{c}} \cdot [\mathbf{S}_i \times (\mathbf{S}_{i+\delta_2} + \mathbf{S}_{i-\delta_2} - \mathbf{S}_{i+\delta_3} - \mathbf{S}_{i-\delta_3})] , \quad (15)$$

which again does not change the ground state and produces only cubic terms in the bosonic representation of the uniform resonance modes.

Thus, the ESR spectrum in the high-field state can be studied with a simplified two-sublattice representation of the full spin Hamiltonian (9):

$$\hat{\mathcal{H}}_{2s} = 4J' \mathbf{S}_1 \cdot \mathbf{S}_2 + 4D'_b \hat{\mathbf{x}} \cdot [\mathbf{S}_1 \times \mathbf{S}_2] - \mathbf{H} \cdot (\mathbf{S}_1 + \mathbf{S}_2) . \quad (16)$$

Let us emphasize again that the expression (16) is applicable only for studying ESR modes with  $\mathbf{k} = 0$  in the folded Brillouin zone. The saturation field  $H_s$ , which corresponds to magnon condensation at an incommensurate value of  $k_b$  [1], must be obtained from the full spin Hamiltonian (9), see Sec. IV.

## HIGH-FIELD MAGNETIC RESONANCE

We now investigate modes of the ESR resonance for the two-sublattice antiferromagnet with the Dzyaloshinskii-Moriya interaction (16) in the high-field paramagnetic state. In the following, the vector components  $x$ ,  $y$ , and  $z$  refer to the rotated coordinate frame with the  $z$  axis being parallel to the field direction.

### Collinear geometry

Let us begin with the collinear geometry  $\mathbf{H} \parallel \mathbf{D}$ . In this case  $S_{\text{tot}}^z$  is a good quantum number and for  $H > H_s$  all spins become parallel to  $\mathbf{H}$ . Using the standard Holstein-Primakoff transformation and keeping only harmonic terms we obtain for Eq. (16):

$$\hat{\mathcal{H}}_2 = 4J'S (a_1^\dagger a_2 + a_2^\dagger a_1 - a_1^\dagger a_1 - a_2^\dagger a_2) + 4D'_b S i (a_1^\dagger a_2 - a_2^\dagger a_1) + H (a_1^\dagger a_1 + a_2^\dagger a_2) . \quad (17)$$

Straightforward diagonalization yields two resonance modes

$$\varepsilon_{1,2} = H - 4J'S \pm 4S \sqrt{J'^2 + D_b'^2} , \quad (18)$$

such that the splitting between the two resonance modes at any given  $H > H_s$  is

$$\varepsilon_1 - \varepsilon_2 = 8S \sqrt{J'^2 + D_b'^2} . \quad (19)$$

For  $S = 1/2$  and weak DM interactions, the mode splitting is approximately given by

$$\Delta\varepsilon \approx 4J'[1 + D_b'^2/(2J'^2)] .$$

By explicitly writing the diagonalization transformation for Eq. (17) we can also determine the intensity ratio for the two modes. First, one performs the transformation to symmetric/antisymmetric bosons:

$$b_1 = \frac{1}{\sqrt{2}}(a_1 + a_2) , \quad b_2 = \frac{1}{\sqrt{2}}(a_1 - a_2) , \quad (20)$$

which yields

$$\hat{\mathcal{H}}_2 = H b_1^\dagger b_1 + (H - 8J'S) b_2^\dagger b_2 + 4D'_b S i (b_2^\dagger b_1 - b_1^\dagger b_2) . \quad (21)$$

The RF field with  $q = 0$  couples to the symmetric  $b_1$  boson. Hence, the ESR absorption is given by the imaginary part of the transverse uniform susceptibility

$$\chi''(q = 0, \omega) = -\frac{1}{\pi} \text{Im}\{G_1(\omega)\} , \quad G_1(t) = -i\langle T b_1(t) b_1^\dagger \rangle . \quad (22)$$

Subsequent transformation to the eigenmodes (18) is performed with the generalized operator rotation

$$b_1 = u c_1 + i v c_2 , \quad b_2 = u c_2 + i v c_1 , \quad \text{with} \quad u^2 + v^2 = 1 . \quad (23)$$

Choosing

$$2uv = \frac{D'_b}{\sqrt{J'^2 + D_b'^2}} , \quad (24)$$

we arrive at the spectrum (18). The susceptibility on the other hand is given by a sum of two delta-functions:

$$\chi''(\omega) = u^2 \delta(\omega - \varepsilon_1) + v^2 \delta(\omega - \varepsilon_2) . \quad (25)$$

Since  $v \approx D'_b/(2J')$ , the intensity ratio for the two modes scales as

$$I_2/I_1 \sim (D'_b/2J')^2 .$$

### Orthogonal geometry

Now consider the orthogonal geometry  $\mathbf{H} \perp \mathbf{D}$ . In this case the two-sublattice structure,

$$\mathbf{S}_1 = (-\cos \theta, 0, \sin \theta) , \quad \mathbf{S}_2 = (-\cos \theta, 0, \sin \theta) , \quad (26)$$

with  $\theta \rightarrow \pi/2$  survives to arbitrary strong magnetic fields. The classical energy is

$$E_c = -4J'S^2 \cos 2\theta - 4D'_b S^2 \sin 2\theta - 2HS \sin \theta . \quad (27)$$

Its minimum is achieved for

$$\sin \theta - \frac{D'_b}{2J'} \frac{\cos 2\theta}{\cos \theta} = \frac{H}{8J'S} \equiv h . \quad (28)$$

For  $h \gg 1$ , one finds  $\theta = \pi/2 - \alpha$  with  $\alpha \approx D'_b/[2J'(h-1)]$ .

Transforming for each sublattice to the local twisted frame we obtain with the required accuracy

$$\hat{\mathcal{H}}_{2s} = 4J'[S_1^y S_2^y - \cos 2\theta(S_1^x S_2^x + S_1^z S_2^z)] - 4D'_b \sin 2\theta(S_1^x S_2^x + S_1^z S_2^z) - H \sin \theta(S_1^z + S_2^z) , \quad (29)$$

which yields the harmonic magnon Hamiltonian

$$\begin{aligned} \hat{\mathcal{H}}_2 &= A(a_1^\dagger a_1 + a_2^\dagger a_2) + C(a_1^\dagger a_2 + a_2^\dagger a_1) - B(a_1 a_2 + a_2^\dagger a_1^\dagger) , \\ A &= 4J'S + 4D'_b S \tan \theta , \quad B = 4S \cos \theta (J' \cos \theta + D'_b \sin \theta) , \quad C = 4S \sin \theta (J' \sin \theta - D'_b \cos \theta) . \end{aligned} \quad (30)$$

The diagonalization of (30) is somewhat more involved but is still straightforward. It yields two resonance modes

$$\varepsilon_{1,2} = \sqrt{(A \pm C)^2 - B^2} , \quad (31)$$

or, denoting  $d = D'_b/J'$ ,

$$\varepsilon_1 = 4J'S \sqrt{(2 \sin^2 \theta - d \tan \theta \cos 2\theta)(2 + d \tan \theta)} , \quad \varepsilon_2 = 4J'S \sqrt{d \tan \theta (2 \cos^2 \theta + d \tan \theta + d \sin 2\theta)} , \quad (32)$$

They have the following asymptotic expressions

$$\varepsilon_1 \approx H + O(d^2) , \quad \varepsilon_2 \approx H - 8J'S + O(d^2) . \quad (33)$$

Thus, the splitting between the two resonance branches in  $\text{Cs}_2\text{CuCl}_4/\text{Cs}_2\text{CuBr}_4$  is again approximately given by

$$\Delta\varepsilon \approx 4J' + O(d^2) .$$

We emphasize again that despite a small contribution into  $\Delta\varepsilon$ , a finite value of the staggered component of the DM vector  $D'_b$  is essential for observing the weak secondary mode. Its intensity vanishes as  $D'_b \rightarrow 0$ .



## SATURATION FIELD

In the presence of noncollinear DM vectors (9), the calculation of the saturation field for a general direction of the applied field becomes rather cumbersome. Therefore, we restrict ourselves to the experimentally relevant case  $\mathbf{H} \parallel \mathbf{b}$ . This field orientation is also the simplest one from the theoretical point of view as spins become parallel to the field at  $H > H_s$ , see Secs. II and III. For such a collinear spin arrangement it is easy to check that the transverse DM terms with  $D_a$  ( $D'_a$ ) and  $D_c$  ( $D'_c$ ) contribute only cubic bosonic terms after the Holstein-Primakoff transformation and, therefore, do not affect magnon energies in the harmonic approximation. Thus, we need to take into account only the DM term with the longitudinal  $D'_b$  component (14).

Leaving behind the standard steps we note that the representation (14) implies that the  $J'$  and  $D'_b$  bonds simply sum up in the saturated phase. This leads to the replacement  $J' \rightarrow J' + iD'_b$  in the hopping terms in the bosonic Hamiltonian. As a result the magnon energy in the saturated phase is given by a simple generalization of the standard equation

$$\varepsilon_{\mathbf{k}} = H - 4(J + J')S + 4JS \cos^2 \frac{k_x}{2} - 4S \sqrt{J'^2 + D_b'^2} \cos \frac{k_x}{2} \cos \frac{k_y \sqrt{3}}{2}. \quad (34)$$

Minimization of the above expression with respect to  $\mathbf{k}$  yields  $k_y = 0$  and  $\cos k_x/2 = \sqrt{J'^2 + D_b'^2}/2J$ . As a result the saturation field is given by

$$H_s = 4(J + J')S + \frac{J'^2 + D_b'^2}{J} S, \quad (35)$$

which for  $S = 1/2$  yields the expression (8) from the main text.

---

\* Present address: Radboud University Nijmegen, Institute for Molecules and Materials, High Field Magnet Laboratory, 6500 GL Nijmegen, The Netherlands

† Present address: Rutgers Center for Emergent Materials and Department of Physics and Astronomy, Rutgers University, Piscataway, NJ 08854, USA

[1] R. Coldea, D.A. Tennant, K. Habicht, P. Smeibidl, C. Wolters, and Z. Tylczynski, Phys. Rev. Lett. **88**, 137203 (2002).

[2] O.A. Starykh, H. Katsura, and L. Balents, Phys. Rev. B **82**, 014421 (2010).